International Forum on Aeroelasticity and Structural Dynamics
IFASD 2017
25-28 June 2017 Como, Italy

EXPERIMENTAL ASSESSMENT OF THE FLUTTER STABILITY OF A LAMINAR AIRFOIL IN TRANSONIC FLOW

Anne Hebler[1]

[1]DLR - German Aerospace Center
Institute of Aeroelasticity
Bunsenstr. 10, 37073 Göttingen, Germany
Anne.Hebler@dlr.de

Keywords: Flutter Boundary, Experiment, Laminar Airfoil, Transonic Flow, Aeroelastic Stability

Abstract: First results of a flutter experiment in transonic flow are presented. A wind tunnel model with the laminar CAST 10-2 airfoil was mounted elastically with heave and pitch degrees of freedom in the Transonic Wind Tunnel Goettingen. Laser triangulators and acceleration sensors were used to record the motion of the model. Measurements were taken with free and fixed boundary layer transition in a Mach number range of $0.5 \leq Ma \leq 0.85$ and for chord Reynolds numbers of $1.0 \cdot 10^6 \leq Re_c \leq 3.5 \cdot 10^6$. For free transition flutter and limit cycle oscillations occurred both when the model degrees of freedom were structurally coupled and when the degrees of freedom were only aerodynamically coupled. However when the boundary layer transition was fixed at 7.5% chord, flutter occured only in the case of structurally coupled degrees of freedom.

1 INTRODUCTION

Laminar flow technologies have moved into the focus of current research, because they provide an opportunity for the design of more environmental-friendly and eco-efficient aircraft. The lower gradient of the boundary layer velocity profile under laminar flow conditions results in less skin friction and thereby less drag than under comparable turbulent flow conditions. The potential of drag reduction for the whole aircraft due to laminar flow on the wing is estimated at 11%. Large regions of laminar flow on the wing can be accomplished either passively by optimizing the shape of the airfoil or actively by controlling the flow (e.g. boundary layer suction). Currently the aerodybnamic community is putting a lot of effort into the development of natural and hybrid laminar flow control [1]. However, the influence of laminar flow on the wing on the aeroelastic behavior, especially on the flutter stability, is still a point of research. Flow characteristics may change significantly in comparison to modern supercritical airfoils. As flutter can lead to severe damages, it limits the flight envelope of an aircraft. The flutter boundary typically forms a minimum in the transonic flight regime, which is called the transonic dip. The laminar flow also has an influence on the position and shape of this dip. As a result it is necessary to investigate the flutter behavior of a laminar airfoil in the transonic flow regime.

Few experimental flutter investigations exist for laminar airfoils in the literature. Some studies, in which no means of transition tripping was applied, reported oscillations for subsonic attached flow with free transition as well as for transonic flow conditions [2, 3]. For the transition on an airfoil in plunging motion a quasi-steady approximation was used to find an explanation for

the physical mechanism of the measured vibrations [3] and then directly transferred to pitching motion. In contrast to this approach it is stated in [4], that transition on a pitching or plunging airfoil can be delayed or promoted by pressure gradients, unsteady effects of accelerated flow and moving wall effects.

A systematic study of the behavior of an laminar airfoil has been undertaken at the DLR recently. Experimental investigations as well as numerical studies were conducted. In previous forced-motion wind tunnel experiments steady-state polars and pitch oscillations of a two-dimensional CAST 10-2 airfoil model were investigated [5, 6]. The measurements were carried out with the plain airfoil (free transition) and with transition tripping dots at x/c = 0.075 (fixed transition). Nonlinearities in the steady-state behavior of the aerodynamic forces for transitional flow[1] as well as significant differences in the motion-induced unsteady airloads between transitional and fully turbulent flow were observed [6]. Forced heave oscillations were not measured due to technical limitations. In order to prepare this flutter experiment the stability boundary was predicted by means of a Doublet-Lattice Method (DLM) corrected using the forced-motion wind tunnel data [7]. This low fidelity method is showing a more pronounced transonic dip for free transition than for fixed transition.

Furthermore, steady as well as unsteady high fidelity computational fluid dynamics (CFD) calculations were performed for this airfoil in separate studies [8–10]. The laminar drag bucket as well as nonlinearities in the steady polars were determined in the Reynolds-averaged Navier-Stokes (RANS) calculations using a γ-Re_θ transition model. The simulations predicted differences in the unsteady airloads between turbulent and transitional flow. The lower transonic dip for free transition was also observed, but in addition a shift towards lower Mach numbers was reported. Qualitatively, the results of the simulation and the experiment match, however quantitative differences exist. The transition location in the simulation is dependent on the choice of the transition model. On the other hand wall effects influence the results of the wind tunnel experiment. In order to understand the physics of the laminar airfoil during flutter and to provide a database for further CFD investigations, a flutter experiment with the CAST 10-2 laminar airfoil is presented in this paper.

2 EXPERIMENTAL SET-UP

The flutter experiment was designed to determine the stability boundary in the transonic region under fully turbulent flow conditions as well as under free laminar-turbulent transition. The main interest lay on the identification of the influence of the laminar-turbulent transition on the transonic dip.

2.1 Wind tunnel

The experiment was conducted in the Transonic Wind Tunnel Goettingen (TWG), which is operated by the foundation German-Dutch Wind Tunnels (DNW), see fig. 1. The wind tunnel has a closed circuit and can be used with various test sections with cross sections of 1m x 1m and a length of 4.5m. The upper and lower wall of the used test section are adjustable, enabling the walls to be adapted to the steady flow field for each measurement point. For that purpose pressure measurements at both walls are fed into a single-step algorithm, which is based on Cauchy's integral formula. The Mach number and the static pressure can be set to specific

[1] When the boundary layer exhibits a considerable amount of laminar flow.

values independently, whereas the temperature can only be controlled in a certain range. In this investigation measurements were conducted for Mach numbers between 0.5 and 0.85 and at static pressures between 40 kPa and 90 kPa, resulting in Reynolds numbers based on the model's chord length of $1.0 \cdot 10^6 \leq Re_c \leq 3.5 \cdot 10^6$.

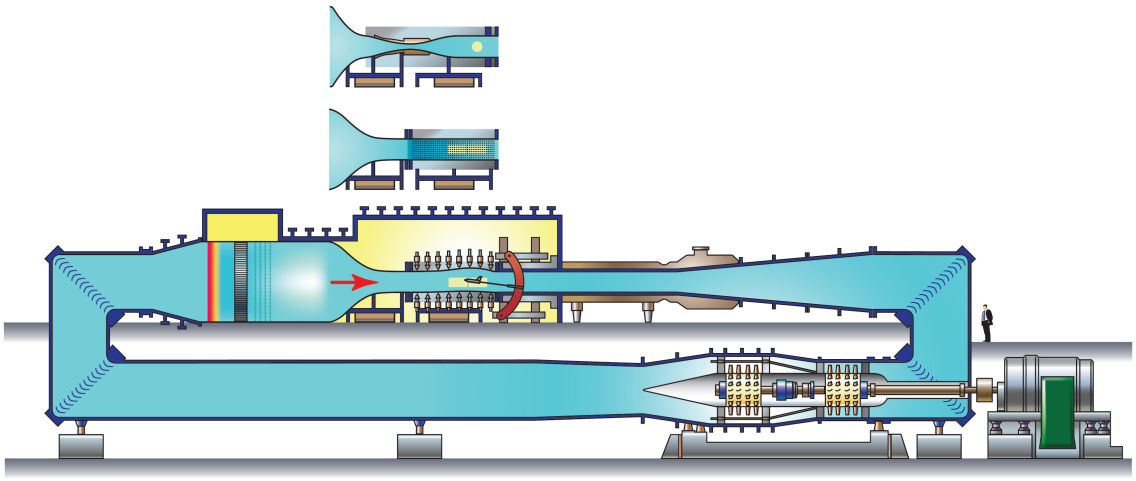

Figure 1: Transonic Wind Tunnel Goettingen. [Source: internal communication DNW]

2.2 Test set-up

For the current experiment the institute's flutter test rig was used, which is shown in fig. 2. It enables the model to be mounted elastically with two degrees of freedom, with torsional cross springs for free pitch motion and pairs of plate springs for free heave motion. Since the test rig is designed for two dimensional airfoil models, the set-up is symmetrical. Between the torsional cross spring and the plate springs a piezoelectric balance with high stiffness has been integrated to measure the aerodynamic forces and moments. Outside the wind tunnel walls a beam has been attached to the model, serving as the target for two sets of laser triangulators, which are used to measure the instantaneous heave and angle of attack. In addition, weights can be fixed at both ends of the beam to change the position of the center of gravity, thereby influencing the eigenfrequencies and the coupling of the eigenmodes. Furthermore a bracket is installed at the beam allowing a pneumatic friction break to stop the oscillations of the model immediately in case of rapid amplitude growth at a flutter point. This brake is either operated manually or it is triggered automatically, when the amplitude of the angle of attack exceeds a preset threshold. The heave motion of the model can be either damped or excited using electrodynamic shakers mounted underneath the plate springs on each side. The input signal for the shakers is generated by a digital signal processing device, which instantaneously computes the heave velocity and its frequency from the signals of the laser triangulators. When this flutter control system is operated in an open-loop state, it does not influence the flutter system [11].

The angle of incidence without wind, the structural dynamic parameters as well as the flow field determine the mean angle of attack of the aeroelastic system. In order to set a specified angle of attack for certain flow conditions, one would have to change the angle of incidence without wind, which can be achieved only with great efforts. Therefore, the whole test set-up is installed to the wind tunnel wall in such a way, that it is possible to rotate the set-up around the elastic axis. This allows an adjustment of the mean angle of attack under wind-on conditions.

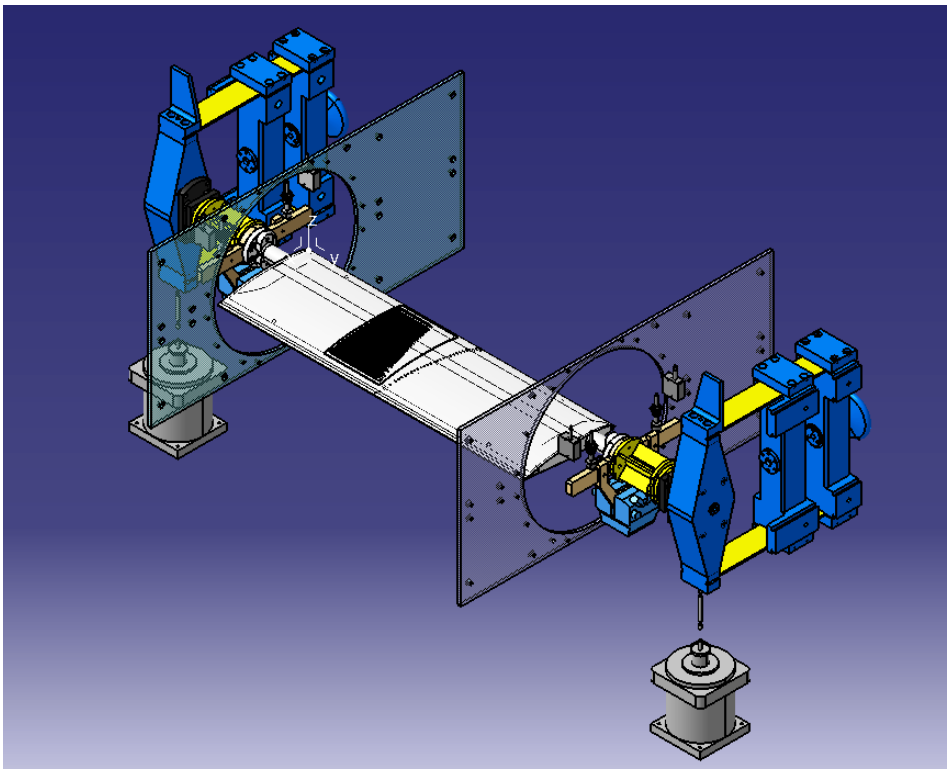

Figure 2: Flutter test rig

2.3 Wind tunnel model and instrumentation

A two dimensional model with the Dornier CAST 10-2 airfoil is used for this investigation. It has a span of $b = 0.997\mathrm{m}$ and its chord length is $c = 0.3\mathrm{m}$. As the model shall be lightweight and stiff at the same time for the flutter investigation, the model is built of carbon fibre-reinforced plastic (CFRP). It consists of two half shells, each of them having a constant lay-up of the laminate in span-wise direction with a thickness of up to $3\mathrm{mm}$. A c-spar, also made of CFRP, at a position of $x/c = 0.33$ increases the stiffness of the model. In order to mount the model to the test rig aluminum connectors are integrated to the half shells at both ends of the model. The connectors permit oscillations about the quarter chord.

The model is equipped with various measurement techniques. 60 unsteady pressure sensors of type Kulite XCQ-093D 5PSI are used to measure the pressure distribution in one central section. The model furthermore contains six accelerometers to measure the motion of the oscillating airfoil. The accelerometers are of type PCB 352C22 and are installed at $x/c = 0.0833$ and 0.8733 in flow direction and at $y/b = 0.15, 0.50$ and 0.85 in span-wise direction. In order to detect the unsteady motion of the laminar-turbulent transition, the model is equipped with 26 hot-film sensors on its suction side to determine the condition of the boundary layer. The sensors capture a range of $0.10 \leq x/c \leq 0.80$ with a spacing of $2.5 - 5.0\%$ of the chord length.

2.4 Structural model

The set-up allows the model to oscillate in two degrees of freedom, heave h and pitch α. A theoretical model of the set-up is depicted in fig. 3. The equations of motion of this system are

$$m\ddot{h} + D_h\dot{h} + K_h h + S_\alpha\ddot{\alpha} = -L \tag{1}$$

$$S_\alpha\ddot{h} + I_\alpha\ddot{\alpha} + D_\alpha\dot{\alpha} + K_\alpha\alpha = M \tag{2}$$

In these equations m is the mass of the flutter system, D_h the damping of heave motion, K_h the stiffness of the plate springs, S_α the static mass moment, I_α the mass moment of inertia, D_α the damping of pitch motion, K_α the stiffness of the torsional springs, L the lift force and M the pitching moment. The elastic axis is located at the quarter chord. The distance of the center of gravity to the elastic axis is $x_\alpha c$.

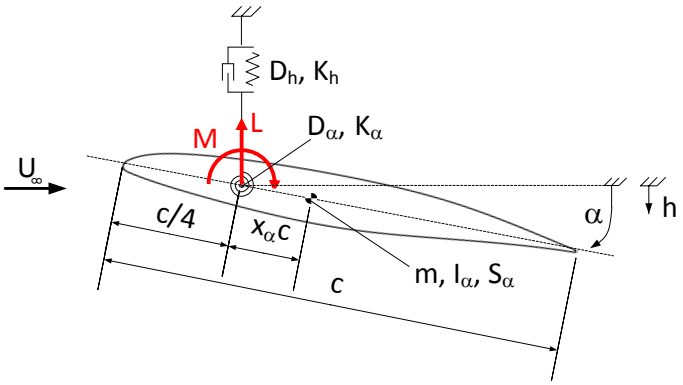

Figure 3: Theoretical model of the flutter system

During the experiment two different structural configurations were investigated. For the first configuration the model was balanced about its quarter chord, such that the center of gravity lies on the elastic axis, resulting in $x_\alpha = 0$ and $S_\alpha = 0$. This means that the two modes are coupled by the aerodynamic forces only. Additional weights, each of about 0.65kg, were attached to the beam for this purpose. For the second configuration the center of gravity is located behind the elastic axis, realized by removing the additional weights. In this case the modes are coupled aerodynamically as well as elastically. The structural parameters of both configurations can be found in table 1. A ground vibration test (GVT) was performed to analyse the frequencies and dampings of the system.

Parameter	Symbol	Unit	Config. 1	Config. 2
Mass	m	kg	27.566	26.252
Mass moment of inertia	I_α	kg/m^2	0.1092	0.0776
Torsional spring stiffness	K_α	N m/rad	$7.282 \cdot 10^3$	$7.282 \cdot 10^3$
Leaf spring stiffness	K_h	N/m	$8.902 \cdot 10^5$	$8.902 \cdot 10^5$
Static moment	S_α	kg m	0.0	0.2659
Structural torsional damping	γ_α	%	1.28	1.47
Structural heave damping	γ_h	%	1.62	1.78
Pitch frequency	f_α	Hz	41.1	50.4
Heave frequency	f_h	Hz	28.6	27.3

Table 1: Structural parameters of the CAST 10-2 wind tunnel model in the flutter test rig

2.5 Data acquisition

All signals were recorded with a DEWETRON data acquisition system that encompasses a 24bit Delta-Sigma A/D converter for each channel. The unsteady pressure and the accelerometer signals from the model as well as unsteady pressure signals from the wind tunnel top and bottom walls were sampled at a fixed sample rate of $F_S = 1200\text{Hz}$. A fixed sample rate of $F_{S_{hf}} = 120\text{kHz}$ was used to record the signals from the hot-film sensors. Steady mean data

from the wind tunnel, like the positions of the adaptive walls, the steady wall pressures, Mach number, total temperature, total pressure and static pressure are measured separately for each measurement point.

2.6 Measurement program

Measurements were taken for the two different structural configurations, both with free boundary layer transition and with fixed transition. For a certain angle of attack a constant static pressure was set in the wind tunnel and the flow velocity was increased stepwise. This was continued until the flow separated from the trailing edge. This was repeated for several (2 to 6) different static pressures, depending on the measured response. Stable as well as unstable conditions were recorded.

In order to keep the angle of attack constant while the Mach number is increased, the test rig can be rotated with α_{2D} about the elastic axis. If the test rig is rotated about the elastic axis, the heave direction with respect to the flow direction is altered as well. For the measurements with a desired mean angle of attack of $\alpha_0 = 0.0°$ the angle of the test rig was $-0.1° \leq \alpha_{2D} \leq 1.78°$. This led to an error in the heave direction of less than 0.05%. As the lift polars are nonlinear (see fig. 4), it is important to keep the angle of attack constant, therefore a deviation in the heave direction is accepted. An overview of the test cases measured is given in table 2.

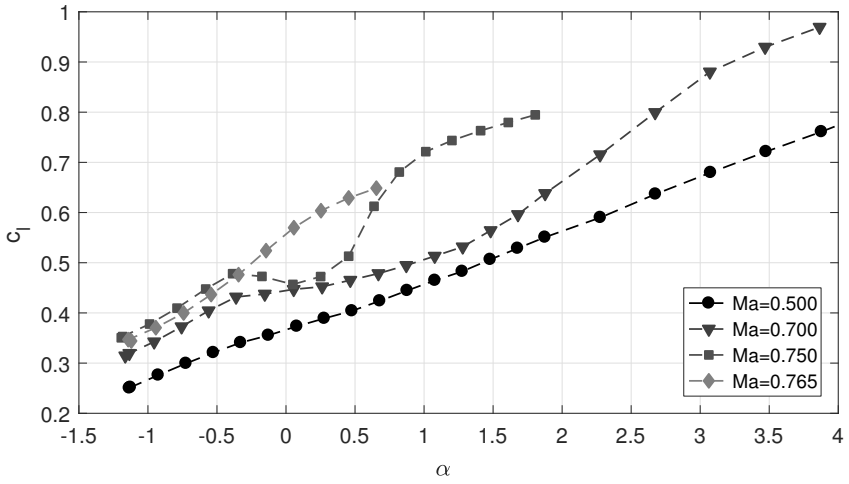

Figure 4: Lift polars for CAST 10-2 with free transition

	free transition		fixed transition	
angle of attack in °	config. 1	config. 2	config. 1	config. 2
-0.8	✓	x	x	x
0.0	✓	✓	✓	✓
0.8	✓	x	x	✓

Table 2: Overview of measurements

3 RESULTS

3.1 Configuration 1

3.1.1 Free Transition

For free transition and the first structural configuration, i.e. aerodynamical coupling only, three different mean angles of attack were chosen for the flutter investigation. Around the angle of attack of $\alpha_0 = -0.8°$ the lift polars are linear for all measured flow conditions (fig.4). In the experiment no flutter instabilities occured. Figure 5 shows the progression of frequency and damping of heave and pitch over the investigated Mach number range for two static pressures. The frequencies stay nearly constant over the whole Mach number range. More fluctuations are found for the damping, but it is positive and thus stable for nearly all test cases. Only at $Ma = 0.815$ the system becomes unstable. The mean pressure distribution at $Ma = 0.815$ and $p_0 = 80\text{kPa}$ is shown in fig. 6. The errorbars mark a confidence interval (CI) of the pressure coefficient of 95.4%. A strong shock has formed on the pressure side. On the suction side the pressure sensors show large fluctuations downstream of $x/c = 0.55$. The pressure coefficient at the trailing edge becomes negative during the oscillations, indicating separated flow. Therefore, the instability at $Ma = 0.815$ refers to boundary layer separation from the trailing edge, not to a flutter instability.

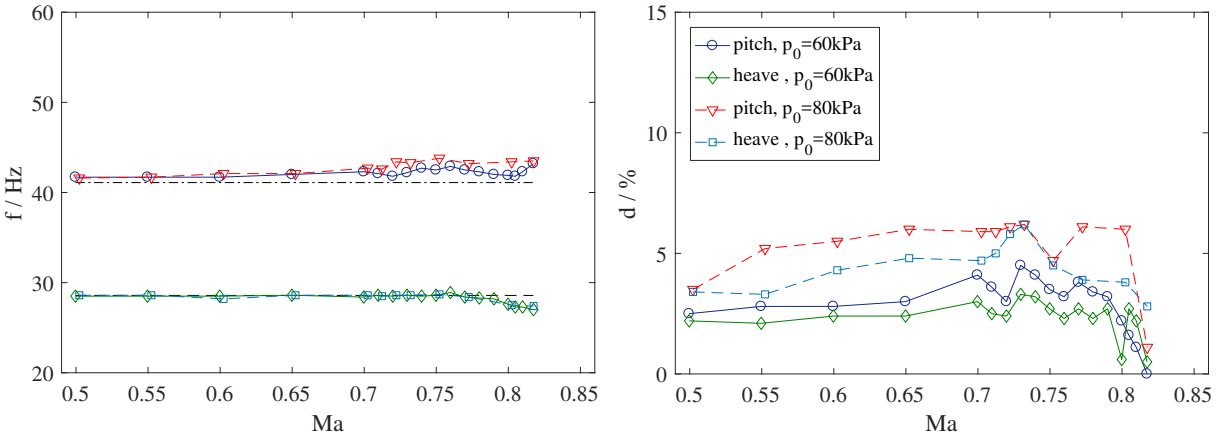

Figure 5: Frequency and damping over Mach number, $\alpha_0 = -0.8°$, free transition, config. 1. The dashed black lines represent the frequencies measured in the GVT without flow.

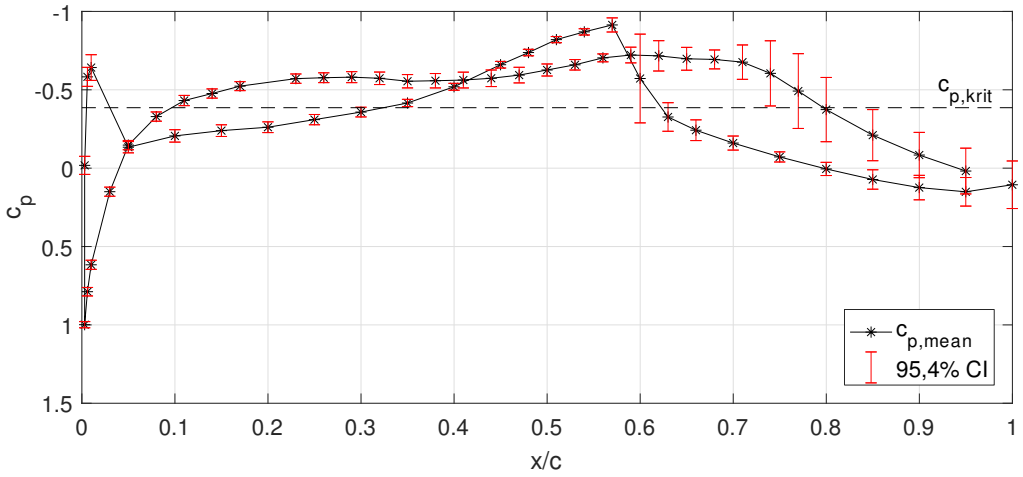

Figure 6: Pressure distribution at $Ma = 0.815$

For measurements in the nonlinear region of the lift polars the mean angle of attack is increased to $\alpha_0 = 0.0°$. For free transition several instability points are found as shown in fig. 7. The wind tunnel model carries out limit cycle oscillations (LCO) in a Mach number range of $0.73 < Ma \leq 0.77$. These LCOs are composed of a large pitching oscillation and only a small portion of heave. Figure 8 depicts the phase planes for $Ma = 0.75$, $p_0 = 70\text{kPa}$ and $\alpha_0 = 0.0°$, illustrating the bounded amplitudes of the instability. The pitch amplitude of the LCO is $\Delta\alpha = 0.311°$, the heave amplitude is $\Delta h = 0.145\text{mm}$ which corresponds to an pitch amplitude of $\Delta\alpha = 0.012°$. The frequencies of the pitch and heave oscillations are the same, in this case $f_p = f_h = 55.83\text{Hz}$. Additional instabilities were found for $Ma \geq 0.81$, which can be attributed to flow separation at the trailing edge, as discussed before.

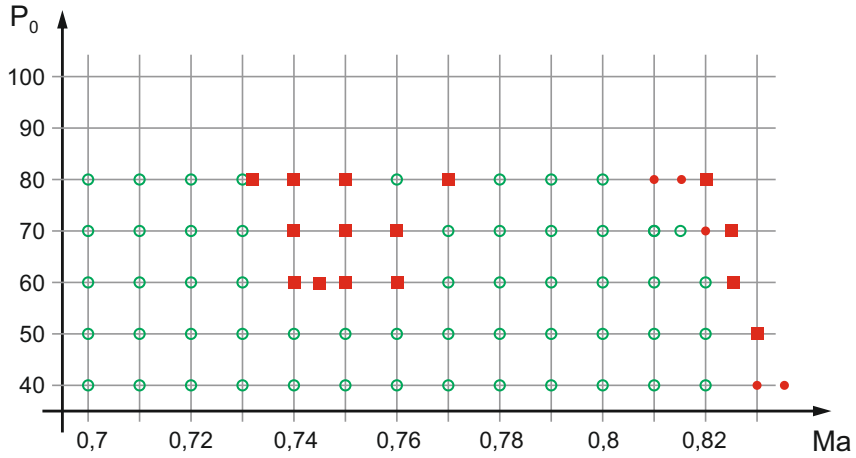

Figure 7: Flutter Boundary (free transition, $\alpha_0 = 0.0°$). Green circles: model is stable. Red dots: increased vibrations, red squares: instabilities were measured.

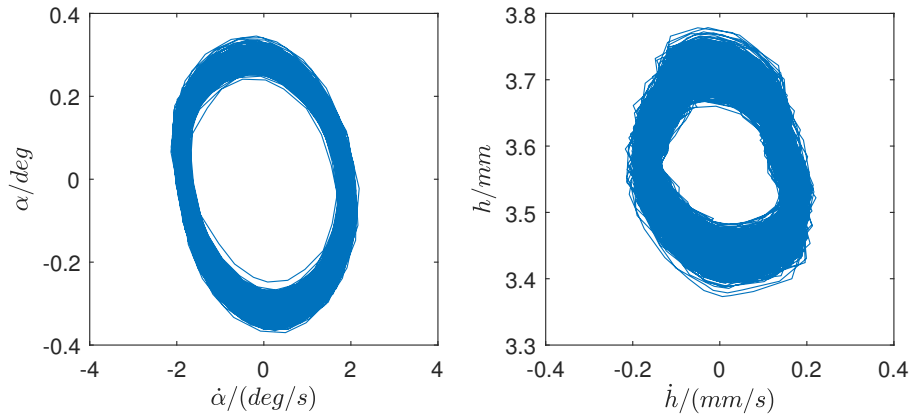

Figure 8: Phase planes for $Ma = 0.75$, $p_0 = 70\text{kPa}$ and $\alpha_0 = 0.0°$

A third mean angle of attack of $\alpha_0 = 0.8°$ was investigated, as the aerodynamic derivatives indicate one degree of freedom flutter at $Ma = 0.75$ [6]. The measured instability diagram is shown in fig. 9. In this case the transonic dip is deeper and somewhat narrower compared to $\alpha_0 = 0.0°$. At $Ma = 0.75$ and $p_0 = 40\text{kPa}$ a limit cycle oscillation with a pitching amplitude of $\Delta\alpha = 1.24°$ and an amplitude in heave of $\Delta h = 0.43\text{mm}$ (corresponding to $\Delta\alpha = 0.027°$ builds up. The amplitude spectra of heave and pitch of this measurement are shown in fig. 10. Both degrees of freedom oscillate with a frequency of 43.54Hz, which is close to the off-wind pitch frequency of 41.1Hz. The off-wind heave frequency of 28.6Hz is also present in the heave data, but the amplitude is more than a magnitude lower.

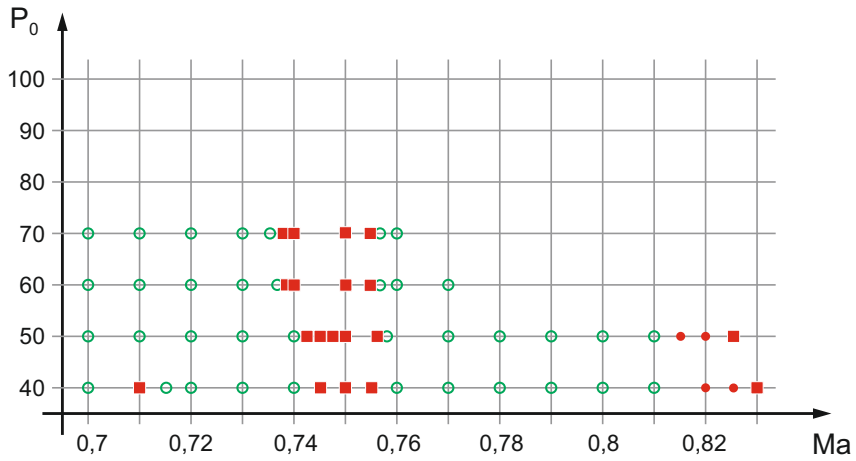

Figure 9: Flutter Boundary (free transition, $\alpha_0 = 0.8°$). Green circles: model is stable. Red dots: increased vibrations, red squares: instabilities were measured.

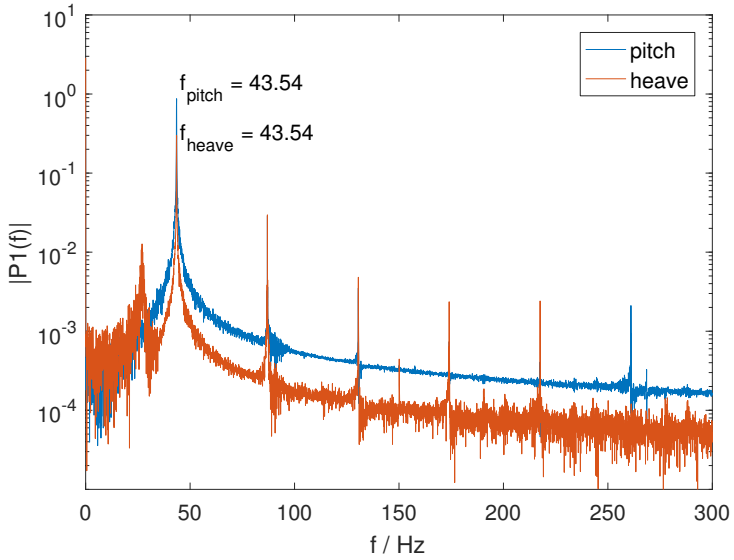

Figure 10: Single-sided amplitude spectrum of heave and pitch signals for $Ma = 0.75$, $p_0 = 40\text{kPa}$ and $\alpha_0 = 0.8°$

3.1.2 Fixed Transition

In order to evaluate the results of the laminar flow, measurements were taken for the same wind tunnel model with fixed transition. For this purpose tripping dots of 0.1270mm height were glued to the suction side and tripping dots of 0.0889mm height to the pressure side of the model, both at a location of 7.5% of the chord. In former investigations with the same model it was shown, that those trippings were sufficiently high to initiate transition. A mean angle of attack of $\alpha_0 = 0.0°$ was chosen. For static pressures of $p_0 = 70\text{kPa}$ and $p_0 = 90\text{kPa}$ no flutter instabilities were found for fixed transition, except for the instabilities caused by the trailing edge separation, see the squares in fig. 11.

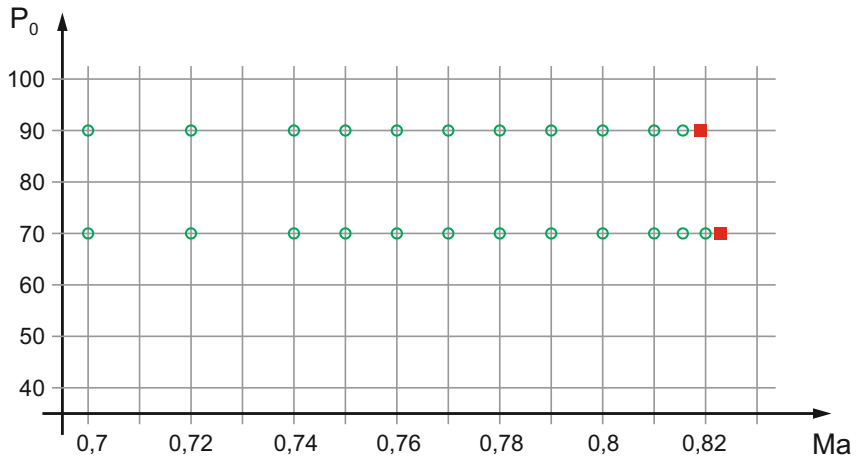

Figure 11: Flutter Boundary (fixed transition, $\alpha_0 = 0.0°$). Green circles: model is stable. Red squares: instabilities were measured.

3.2 Configuration 2

For the second configuration the center of gravity was located behind the elastic axis. Figure 12 shows the stability diagram for free transition at $\alpha_0 = 0.0°$. Flutter instabilities are observed for free transition for $0.73 \leq Ma \leq 0.78$. For this structural configuration, flutter cases with unbounded amplitudes in heave and pitch occurred in addition to LCOs with bounded maximum amplitudes. The heave signal of the measurement at $Ma = 0.757$ and $p_0 = 55\text{kPa}$ as well as the phase plane are shown in fig. 13. The amplitude rises progressively up to $\Delta h = 2.643\text{mm}$, at which point the pneumatic friction brake is closed.

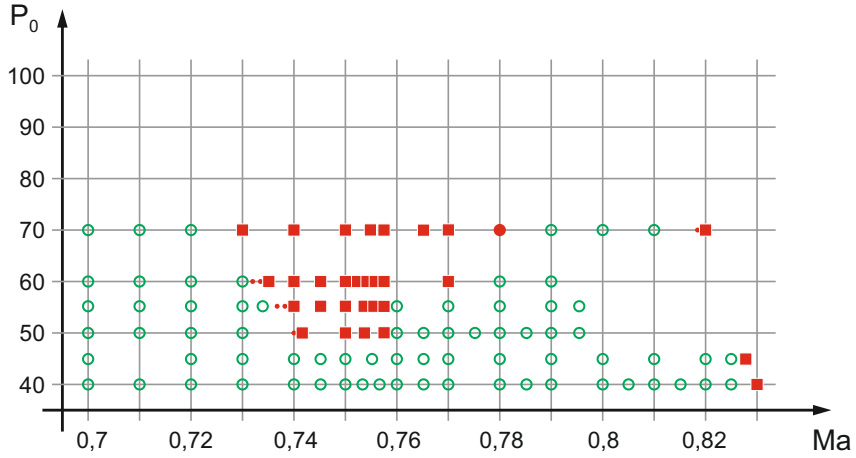

Figure 12: Flutter Boundary (free transition, config. 2, $\alpha_0 = 0.0°$). Green circles: model is stable. Red dots: increased vibrations, red squares: instabilities were measured.

For this structural configuration a transonic dip develops for fixed transition as well, shown in fig. 14. Flutter instabilities are measured for $0.75 \leq Ma \leq 0.80$, beginning at static pressures of $p_0 = 70\text{kPa}$. Comparing the extent of the transonic dip to the one with free transition, one can see that it is shifted to higher Mach numbers and higher static pressures.

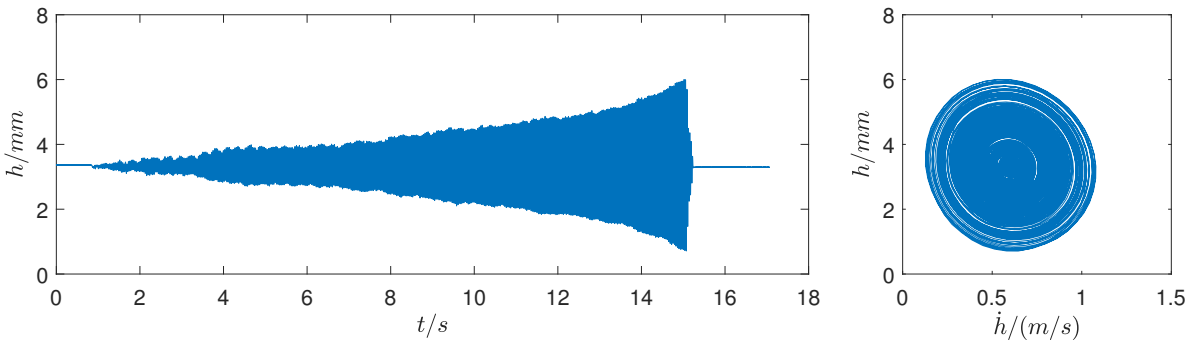

Figure 13: Heave signal for $Ma = 0.757$, $p_0 = 55\text{kPa}$ and $\alpha_0 = 0.0°$. Left: Time series, right: Phase plane

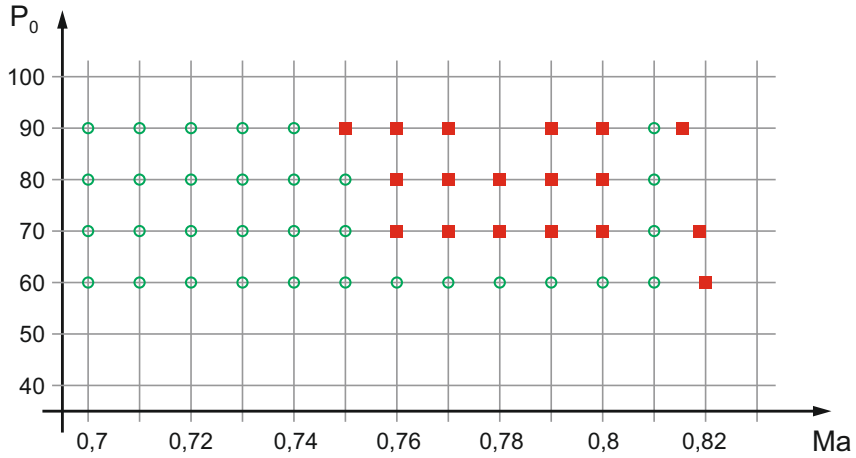

Figure 14: Flutter Boundary (fixed transition, config. 2, $\alpha_0 = 0.0°$). Green circles: model is stable. Red squares: instabilities were measured.

4 CONCLUSION

The flutter stability of the laminar airfoil CAST 10-2 was investigated for two structural configurations. The measured results show substantial differences between transitional and fully turbulent flow.

First, for purely aerodynamic coupling between the heave and pitch degrees of freedom, flutter instabilities exist only when the boundary layer is allowed to transition freely from laminar to turbulent. The wind tunnel model remains stable for fixed transition. This is in agreement with flutter calculations using DLM corrected with wind tunnel data [12]. It appears that the presence of the laminar boundary layer introduces an aerodynamic nonlinearity into the system, which causes the limit cycle oscillations.

A variation of the angle of attack for free transition was also presented for this structural configuration. No flutter instabilities occurred for the smallest angle of attack. With increasing angle of attack limit cycle oscillations start to appear. The frequency of the LCOs differs for the two larger angles of attack. At the highest angle of attack LCOs form with pitch as the prominent degree of freedom. While the results for the low and high angle of attack are in accordance with the previous numerical studies [12], no LCOs were predicted for the medium angle of attack. However, in the forced motion experiment the lift derivatives exhibit an aerodynamic resonance at $Ma = 0.75$ ([6]), which may be the cause for the LCOs. Further investigations are required.

Second, when structural coupling between the two degrees of freedom is added, flutter instabilities are present for both free and fixed transition cases. The transonic dip is deeper and

shifted towards lower Mach numbers for the free transition case, which matches qualitatively with previous CFD calculations [9, 10]. However for the fixed transition case, a wider transonic dip is observed. In addition the flutter mechanisms of free and fixed transition cases differ. With free transition limit cycle oscillations as well as flutter with rapidly growing amplitudes exist, whereas with fixed transition only rapidly growing amplitude flutter cases are present.

It can be concluded, that the laminar-turbulent boundary layer transition has a strong influence on the flutter behavior of the CAST 10-2 airfoil. A detailed analysis of the processes in the boundary layer using the data of the hot-film sensors is needed in order to explain the observed behavior.

ACKNOWLEDGMENTS

The measurements were carried out within the DLR project ALLEGRA (AeroeLastic stability and Loads prediction for Enhanced GReen Aircraft). Further evaluation of the data is part of the EU project NACOR. I would like to thank everyone, who contributed to the experiment: Holger Mai, Johannes Nuhn, Thomas Büte, Christian Stieg, Nils van Hinsberg, Stefan Koch, Goran Jelicic and Jan Schwochow.

5 REFERENCES

[1] Green, J.E, *Laminar Flow Control - Back to the Future?*, 38th Fluid Dynamics Conference and Exhibit, 23 - 26 June 2008, Seattle, Washington, AIAA 2008-3738.

[2] Houwink, R., Kraan, A.N., and Zwaan, R.J., *Wind-tunnel Study of the Flutter Characteristics of a Supercritical Wing*, Journal of Aircraft, Vol. 19, pp.400-405. (1982)

[3] Mabey, D.G., Ashill, P.R., and Welch, B.L., *Aeroelastic Oscillations Caused by Transitional Boundary Layers and their Attenuation*, Journal of Aircraft, Vol. 24, pp.463-469. (1987)

[4] Ericsson, L.E., *Transition Effects on Airfoil Dynamics and the Implications for Subscale Tests*, Journal of Aircraft, Vol. 26, pp.1051-1058. (1989)

[5] Mai, H., Hebler, A., *Aeroelasticity of a laminar wing*, Proceedings of the International Forum on Aeroelasticity and Structural Dynamics, IFASD 2011, Paris, France (2011)

[6] Hebler, A., Schojda, L., Mai, H., *Experimental Investigation of the Aeroelastic Behavior of a Laminar Airfoil in Transonic Flow*, Proceedings of the International Forum on Aeroelasticity and Structural Dynamics, IFASD 2013, Bristol, England (2013)

[7] Hebler, A., Thormann, R., *Flutter Prediction of a Laminar Airfoil Using a Doublet Lattice Method Corrected by Experimental Data*, New Results in Numerical and Experimental Fluid Mechanics X: Contributions to the 19th STAB/DGLR Symposium Munich, Germany, 2014, 445-455 (2016)

[8] Fehrs, M., *Influence of Transitional Flows at Transonic Mach Numbers on the Flutter Speed of a Laminar Airfoil*, Proceedings of the International Forum on Aeroelasticity and Structural Dynamics, IFASD 2013, Bristol, England (2013)

[9] Fehrs, M., van Rooij, A. C. L. M., Nitzsche, J., *Influence of boundary layer transition on the flutter behavior of a supercritical airfoil*, CEAS Aeronautical Journal, Volume 6, Issue 2, pp 291-303 (2015)

[10] A. C. L. M. v. Rooij and W. Wegner. Numerical investigation of the flutter behaviour of a laminar supercritical airfoil. In A. Dillmann et al., editors, New Results in Numerical and Experimental Fluid Mechanics IX, number 124 in Notes on Numerical Fluid Mechanics and Multidisciplinary Design, pages 3341. Springer International Publishing, Jan. 2014.

[11] Dietz, G., Schewe, G., Mai, H., *Amplification and Amplitude Limitation of Heave/Pitch Limit-Cycle Oscillations Close to the Transonic Dip*, Journal of Fluids and Structures 22, 505-527 (2006)

[12] Hebler, A., *Vorhersage der Stabilitätsgrenze eines Laminarprofils mit einer Doublet-Lattice-Korrekturmethode basierend auf instationären Versuchsdaten*, Diploma thesis (2014)

COPYRIGHT STATEMENT